History of Medicine:Vol.08 No. 2 (2022):725-735
DOI: https://doi.org/10.48047/HM.08.2.2022.725-735

Reliability and Validity analysis of Tendon morphology assessment during repeated cyclic loading

Anas K. Al Makhzoomi[1*], Garry. T Allison[2], Mohammad S. Khalifeh[1,3], Omran H. Alameri[1]

[1]Department of Veterinary Basic Medical Science, Jordan University of Science and Technology, Irbid, Jordan
[2]Associate Deputy Vice Chancellor - Research Excellence – Curtin University, Perth, Western Australia, Australia.
[3]Department of Molecular Biology and Genetic Engineering, Science College, Jordan University of Science and Technology, Irbid-22110, Jordan
Running title: Reliability and Validity analysis of Tendon morphology

*Corresponding Author: akalmakhzoomi1@just.edu.jo

ABSTRACT
Background: The multi-scale form and function of biological tissues are domains of interest for clinicians and biologists. Common ordinal categorical assessments are widely used in the observational and histological evaluation of tissues. Ordinal scales are commonly reported in the literature, yet few studies report the reliability of the assessors' classification. **Objective:** The development of digital algorithms often relies on the ordinal construct of the original scales with the assumption that the validity of the digital algorithm is self-evident as derived from the valid observational scale. **Methodology:** The experimental methodology included testing White New Zealand Rabbit Achilles tendons at 3%, 6%, 9%, and 6% strain GAG-depleted tendons. Tendon stiffness and morphological changes were assessed at multiple scales with digitally imaged liner modulus and atomic force microscopy. Test-retest protocols and statistical analysis were done with Weighted Kappa to ensure reliability. **Results:** Findings have shown almost perfect within tester and substantial agreements of ordinal classifications (weighted Kappa > 0.98 and > 0.77). The classifications demonstrated a clear dose-response, i.e., more significant damage with increased tendon strain and repetitions. The specific finding emphasizes that the loss of tenocyte spindle-shaped is highly associated with loss of tendon stiffness, whereas other circularity classifications (e.g. Elongated) add little further information. Digital assessment of anisotropy did not demonstrate a dose-response after the initial preconditioning. Therefore, the testing properties of scales for tendon morphology require reporting of both validity (esp. new algorithms) and reliability**. Conclusion:** Furthermore, digital algorithms may improve data reliability and statistical robustness as a continuous variable but still require validation.

Keywords: Tendon Morphology, Cyclic Loading, Ordinal Scales, Reliability Analysis Digital Imaging, Anisotropy Assessment

1. INTRODUCTION

The reliability and validity of the assessment of tendon morphology in response to cyclic loading must be subcritical to actualizing the tendon's adaptability to mechanical stress (1). Specifically, cyclic loading is described as the kind of loading those cycles tendons through repeated cycles of flexing and contracting to mimic athletic use or physical rehabilitation (2). Hugh *et al.* (2018) investigated the use of ultrasound to evaluate shifts in tendon dimensions such as thickness, cross-sectional area, and stiffness of tendon thickness, yielding an interclass correlation coefficient (ICC) of 0.90, arguing reliability (3). In addition, validity is ascertained from comparisons of these ultrasound evaluations against MRI or direct biomechanical assessment, where, more often than not, such correlations are above 0.85, thereby confirming the validity of tendon adaptations under cyclic loading (4). This research explicitly assesses tendon morphological classification using recognized ordinal scales and two digital constructs that are thought to determine similar domains.

Before the technological improvements, tendon characterization is mainly based on morphological classifications such as fibre orientation and arrangement (5-6), fibre structure (waviness) (7-8) and also tenocyte shape (9-12). These classifications are widely employed to describe objectively tendon morphology under different mechanical loading profiles and pathologies (14-17). The statistical basis of the characteristic four scoring points– see Table 1, have inferred validity based on their use across a body of literature (19-22). Yet, there are limited assessments of their validity. No reliability (within or between observers) studies are reported, suggesting that measurement bias accounted for some of the variability within the literature.

The long spindle-shaped tenocytes, observed in unloaded tendons, exhibit columnar arrangement in longitudinal rows aligning between the highly parallel fibres (22). Thorpe *et al.* (2015) literature shows that damage progression reflects changes in the shape towards a greater population of rounder tenocytes (11). On the four-

point classification, the change from long-spindle is objectively defined as slightly, moderately and severely rounded (19-22).

Multi-scale image analysis allows a digital representation for objective assessments of the target tissues. These techniques have issues in the selected images and the region of interest (ROI). In publications, the provided images are often 'exemplars" of what would be expected. Interestingly, digital image processing has improved the ability to assess tendon morphological domains. However, the basic construct of the four-point ordinal classification has influenced the application of these tools. Schöchline *et al.* (2014) elaborated that digital imaging was used to model the degree of roundness of cell (cancer) shape. Still, this continuous variable was converted to an ordinal four-point scale (24).

The cell shape was found to be pathognomonic, and a roundness scale was used to provide four categories. However, these continuous variables (between 0.0 and 1.0) are based on the analysis of the extracted image cell shapes by using the tool kit of the image J -plug-in "Circularity" (24). Thresholds reflected the four-point categories: Spindled, Elongated, Oval and Round. There is no sensitivity analysis if the thresholds' context of these four categories is outside the carcinoma classification. Although the validity and sensitivity of cancerous cells create binary assessments, the tendon morphology does not seem to create the same. Therefore, it is necessary to identify a functional variable that is repeatable and sensitive to changes in repeated mechanical loading. In this context, a normalized decline in tendon stiffness may be the functional marker for testing the morphological scales.

Furthermore, two digitally derived variables that created continuous analogues of the ordinal scales for tenocyte shape and anisotropy will test the concurrent validity of mechanical failure assessment. This research aims to report the reliability of standard operating procedures for objective classifications and to direct future algorithm changes that may require more sensitive assessments of tendon morphology. These aspects will improve the quality of studies and may provide insights into the underlying aetiology of tendon injury.

2. METHODS

2.1 Experimental Approach to the Problem

The experimental methodology involves employing White New Zealand Rabbit Achilles tendons to examine how tendon ultrastructure correlates with mechanical performance following cyclical loading. The study design includes two key experiments: r, one normal tendon was tested at 3%, 6% and 9% strain, and the other was tested after GAG depletion at 6% strain only. These strain levels act as the independent variables concerning which dose-response effects on structures and functionality of tendons can be assessed. Measures of dependent variables are tendon stiffness, fibre structure and morphology of tenocytes using digital images, confocal arthroscopic images and atomic force microscopy. This multi-scale assessment allows investigators to track changes (e.g., anisotropy and circularity of tenocytes) and correlate these to functional parameters such as tendon stiffness. Cohort concordance or test-retest measurements are provided statistically through Weighted Kappa, making the test more reliable and valid (25). The current design offers a way to validate hypotheses concerning the relationship between tendon morphological features and mechanical performance during cyclic solicitations.

2.2 Tendon Preparation and Mechanical Loading

Initially, two independent studies of White New Zealand Rabbit Achilles Tendons underwent repeated cyclic loading in un-depleted tendons at 3%, 6% and 9% strain levels (26, 27) and of GAG-depleted tendons at 6% strain level (28-29). In brief, 720 preconditioning cycles (at 1Hz) images were recorded by a confocal arthroscope (CA). The attached arthroscopic probe to the surface of the tendon allowed at least four images to be taken every 6 minutes (after 240 cycles of repeated cyclic loading). At the end of each hour (2400 cycles of the mechanical testing), various parts of the mid-substance of the tested tendon were prepared for histological sections and then assessed using the Slide Viewing Software (Aperio ImageScope – Leica Microsystems Pty Ltd). Atomic Force Microscopy (AFM) also prepared and evaluated other cryo-sections. These allowed for multi-scale assessments of morphological changes over repeated strain cycles.

2.3 Functional Changes (Dose Response and Tendon Stiffness)

The validity of morphological (form) assessments in the relationship between form and function requires a reliable and sensitive evaluation of function that needs to be well established. The first validation process was to observe a 'dose-response' measured by the ordinal scales. This means that changes in morphology would reflect an increase in the mechanical stimulus dose (in this case, repeated cycles at three strain levels: 3%, 6% and 9% (26, 27). The second functional variable was normalized tendon stiffness. In this case, the derived variable was reliable and sensitive to GAG deletion **(Figure 1)**.

2.4 Ordinal Scales

The four-point ordinal scales **(Table 1)** were used to grade images taken by CA. These included:

1) Fibre structure
2) Fibre orientation and arrangement
3) Tenocyte shape

Table 1. Modified scoring system for Fibre structure, orientation and arrangement and Tenocyte shape (see supplementary information for images)

1. Fibre structure	
A. Continuous and long fibres with no interruption	4
B. Slight separation and fragmentation of fibres, waviness	3
C. Marked waviness, separated and fragmented fibres	2
D. Increased waviness, separated and fragmented fibres	1
2. Fibre arrangement and orientation	
A. Compacted, parallel, regular and well-ordered	4
B. slightly loose and wavy	3
C. Increased loose, wavy and cross to each other	2
D. Moderately loose, wavy crossing each other with some unidentified pattern	1
3. Tenocyte shape	
A. Long spindle shape cells	4
B. Slightly rounding	3
C. Moderately rounding	2
D. Severely rounding	1

4) ***4= normal appearance, 3 = slightly abnormal appearance, 2= moderately abnormal appearance, 1 = severely abnormal appearance.***

2.5 Digital imaging processing Tenocyte shape and Anisotropy

The circularity of the identified cells was determined from the digital images and categorized into four classifications: *Spindled*, circularity values > 0–0.35 Elongated, circularity ≥ 0.35–0.6, *Oval*, circularity ≥ 0.6–0.8 and *Round*, circularity ≥ 0.8–1.0. Schochlin *et al.* (2014) study used the plug-in model of Image J ("Circularity"). Anisotropy of the fibres was determined using the plug-in "FibrilTool" – to generate a score between 0 and 1.0. [0 for no identifiable pattern (purely isotropic fibers) and 1 for parallel, regular and well-ordered fibers (purely anisotropic fibers) (24b). (See detailed methods and images in the supplementary information).

2.6 Reliability Protocol of Categorical Assessments

For categorical data (Table 1), Weighted Kappa for test-retest was calculated. Briefly, a sample of images (120+) representing the range of testing duration was sent to an independent researcher who randomly selected 58 images. Then, these images were replicated and renamed using a random code. In the replicated sample, the images were manipulated further to reduce the chance of visual memory of the image. This included at least two of the following three digital image manipulations – 1) Rotation +/- 90 or 180 degrees, 2) reflection and 3) Change of the image contrast (+/- 20%).

The assessor was blind to the replication and digital manipulation. The images were assessed in one sitting, without returning to previously assessed images, and the process was repeated one week later. All three classifications for each image were undertaken at one time. A second researcher decoded the classifications to match the paired results. This is provided within and between sessions, as well as reliability assessments of the classification undertaken by the assessor. A second independent assessor also scored the images to generate a between-assessor reliability for the three domains.

2.7 Statistical analysis

Descriptive sampling - Images were sampled from the mid-portion of the tendon with changing ROI. Therefore, the mean percentage of each classified (cell shape) or category was recorded ten times per hour. Face validity was determined by assessing each ordinal category's shift (prevalence) against the dose response. The stability of the mechanical changes in the tendon stiffness is demonstrated by mapping three independent study data and reporting the median and upper and lower quartile error bars (16-17). Weighted Kappa (K) with 95% confidence intervals (CI) were used for the within and between tester reliability with the assumption of a linear weighting between categories (30). The validity of continuous variables (the proportion of cells classified by circularity and

anisotropy) was assessed by plotting the change in mechanical function (stiffness) using an XY plot following preconditioning.

3. RESULTS

3.1 Classification Reliability Ordinal Data

The within-testing (blind images) had perfect concordance for all three domains of assessments. For the test-re-test classification, the weighted Kappa was very high (31). Fibre structure (K = 0.972, CI 0.934 – 1.000) is more consistent than fibre orientation and arrangement (K = 0.931, CI 0.873 -0.990). The between tester Kappa had a substantial agreement (K = 0.824 CI 0.742 – 0.907; and 0.766 CI 0.666 – 0.867) with greater agreement with fibre structure. For tenocyte morphology, the intra-tester reliability was very high (near perfect, K = 0.988; CI 0.956 – 1.00). It identified that the definitions of roundness cut-offs for the 4-point classification may be an issue with the relatively lower inter-tester reliability (substantial agreement K = 0.767 CI 0.598 – 0.830).

The data in the graph in Fig 1 shows the variation of tendon stiffness normalized with that of the initial value in the control group A, control group B and GAG deficient group at 6% strain at 2400 cycles per hour. The results demonstrated that the tendons with reduced GAG content revealed a steeper systematic loss of tissue stiffness compared to the control samples. During the time interval of the experiment, all groups are depicted at 100% normalized stiffness at the start of the experiment. However, the stiffness in the GAG-depleted group decreases even more rapidly and reaches only about 40% of its initial level during the 2 hours. At the same time, both control groups, A and B, decline at a slower rate, being 70-80% stiff after 2 hours.

The error bars indicate some dispersion of the data around the median stiffness loss within groups, but the overall picture is easily discernible. The higher reduction rate of the GAG-depleted tendons is owed to the importance of (GAGs) for tendon structure and its ability to withstand stress. As the concentration of GAGs decreases, the rate at which tendons unload their stiffness under cyclic loading increases (figure 1). Furthermore, this result reaffirms the functionality of GAGs in tendon mechanics and the effects that depletion causes. On the other hand, the controls can show better stiffness maintenance, giving an alibi to healthier tendon morphology under such cyclic loading protocols, as shown in Figure 1.

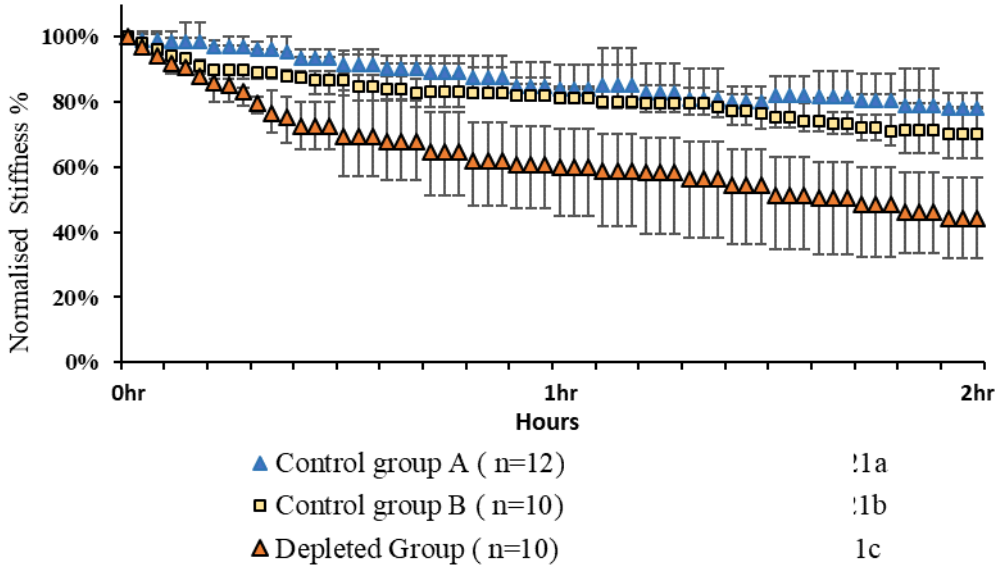

Figure 1: The replication of normalized median (upper and lower quartile) tendon stiffness decline of two control cohorts (n=10 and n=12) and a set of GAG-Depleted (n=10) matched tendons. From two independent experiments, 1, 2. Noting the similar patterns for the controls and the GAG-depletion resulted in more significant stiffness loss with repeated cycles (6% strain @ 2400 cycles every hour).

The findings of this study suggest a high level of inter-observer reliability and variability in cross-sectional assessment of tendon morphology during repeating cyclic loading (figure 2). Within-tester reliability also used a blind image test, which perfectly correlated the evaluated domains, including fibre structure, fibre orientation, and the arrangement of tenocytes and the tenocyte shape. The Weighted Kappa values obtained confirmed high levels of inter-observer agreement across two occasions, indicating adequate test-retest reliability; fibre structure by K = 0.972 showing that the practice had higher reliability than the fibre orientation and its arrangement by K = 0.931. The preceding results imply that it is easier to identify the fibre of structure and that it is stable under cyclic loading of dynamic application. Inter-observer reliability was slightly lower but also significant for fibre structure (K = 0.824), meaning the interpretation of fibre structure is more consistent across testers than for fibre orientation (K

= 0.766). In addition, great intra-tester reliability of tenocyte morphology was found at K = 0.988, which reflects an almost perfect match. However, inter-tester reliability for tenocyte roundness classification was slightly lower with K = 0.767; the cut of values for roundness could be adjusted to show closer concordance between testers (Figure 2). The evaluations show high levels of inter- and intra-inter-rater reliability, which suggest a degree of 'floor' effect in some classification systems.

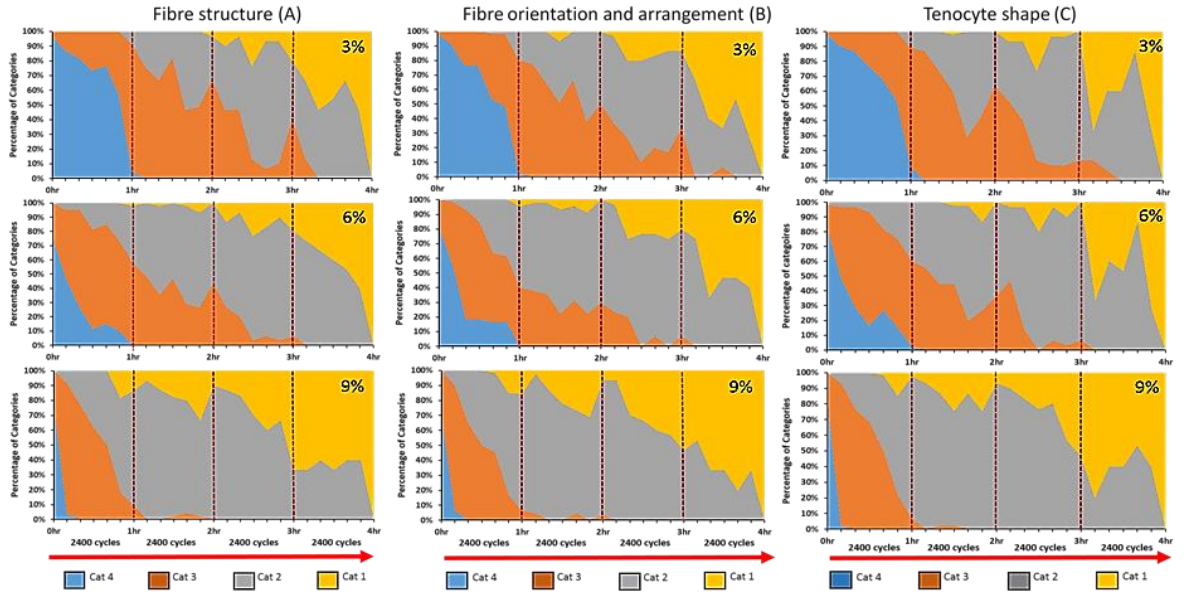

Figure 2: Estimates of percentage allocation of ordinal classification (L to R - Fibre structure (A), Fibre orientation and arrangement(B) and Tenocyte shape (C)) for images taken every 6 minutes (240 cycles) for up to 9600 cycles at three strain levels. Each ordinal classification shows a decline in Category 4 and an increase in each category. This categorical shift in all domains shows a clear "dose-response" for cycles and strain. Note: Each image's region of interest (ROI) does not observe the same cells. Since the tester reliability is almost perfect (Weighted Kappa > 0.9), the variance in the data (including decreases in categories 1 and 2) is explained by the sampling of the different ROI.

3.2 Stability of the mechanical changes (stiffness) during repeated loading

Figure 3 shows the median (upper and lower quartile) percentage decline in tendon stiffness during the 2 hours of the 6% strain for three independent tendons from studies in the same laboratory (26-17). This shows the consistency of the stiffness assessment between different control cohorts - Control A (26) and Control B and the depleted group (27-28). The replicated pattern of the normalized decline in both control groups shows the stability of the reporting protocol. Moreover, the difference between the controls and the GAG data shows that the partial GAG depletion has a more significant difference than the variance between replicated trials. This affirms the magnitude of the mechanical differences in the different cohorts, establishing known differences between groups.

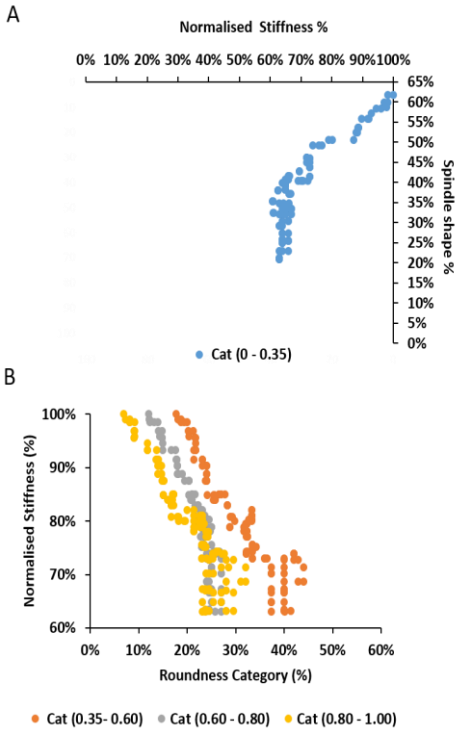

Figure 3: Changes in stiffness vs tenocyte roundness in the 6% strain group over four hours of cyclic loading. A shows the declined proportion of cells with a spindle shape (Cat 4) compared with the declined stiffness. B shows the increase in the proportion of cells in the three remaining categories of roundness (Cat 3, Cat 2 and Cat 1) compared with the declined stiffness.

3.3 Validity of data of ordinal categories during declining tendon stiffness

Figure 4 describes the interaction between tendon stiffness and roundness of the tenocytes during cyclic loading at 6% strain over four hours. **Graph A** shows that as normalized stiffness decreases, there is a decline in cells with a spindle shape (Category 4: Cat 0–0.35). This indicates that although tendons are subjected to mechanical loading and stiffness, only few cells maintain the elongated and spindle-shaped form as expected. This reduction suggests that cellular alterations or degradation occur due to mechanical pressures, forming the basis of the observed decrease in stiffness. Graph B highlights that as tendon (stiffness declines, there is an increase in the proportion of cells with more rounded shapes Cat 0.35–1.00). This raises the question of whether the cells move

from elongated to round shapes due to higher strain, which may indicate mechanical damage or just cell remodelling.

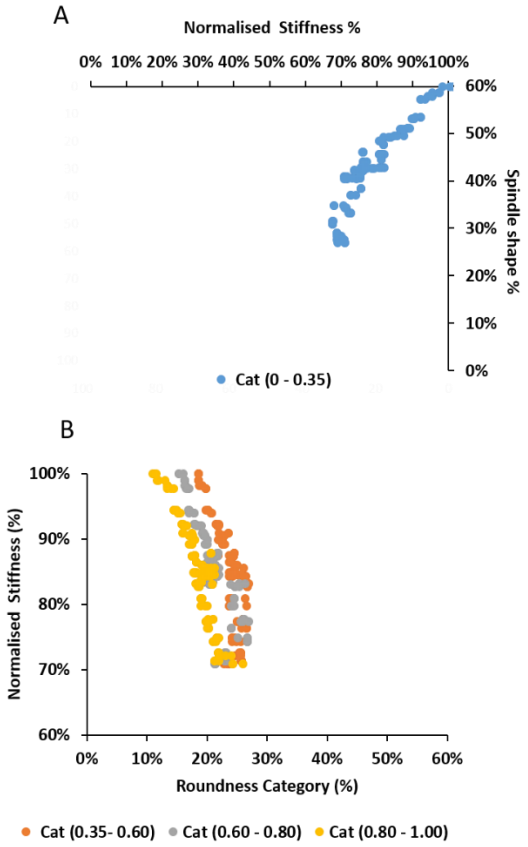

Figure 4: Changes in stiffness vs tenocyte roundness in the 3% strain group over four hours of cyclic loading. A shows the declined proportion of cells with a spindle shape (Cat 4) compared with declined stiffness. B shows the increase in the proportion of cells in the three remaining categories of roundness (Cat 3, Cat 2 and Cat 1) compared with the declined stiffness.

3.4 Objective validation of digital assessments - Tenocyte shape and anisotropy

These graphs in Figure 5 show the tenocyte roundness and normalized stiffness when the cyclic loading was applied at 9% strain for four hours. Graph A shows the decline in normalized stiffness alongside a reduction in cells with a spindle shape (Category 4: Characteristically, Cat 0–0.35 indicating that as tendon stiffness declines, fewer cells retain spindle shape. This suggests that spindle-shaped cells function due to the stiffness of the tendon, and their loss is linked to mechanical deterioration of the tendon. Graph B demonstrates an inverse relationship: instead, with such relaxation; there is a corresponding improvement in the percent of cells in the more rounded categories. This raises the possibility that cells change their shape from elongated functional forms to more spherical forms as the tendon is subjected to mechanical stress. These observations of shrinking diameter are artefacts of increased roundness, presumably a cellular response to the cyclic loading that occurs as the tendon undergoes functional degradation under high strain as a direct response to cyclic loading.

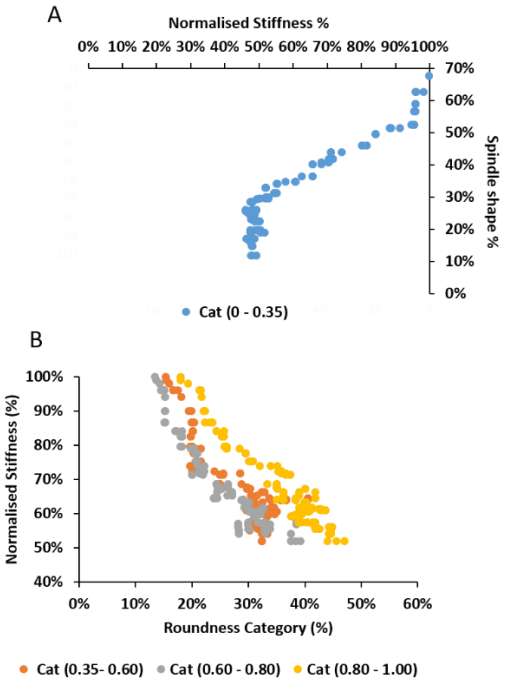

Figure 5: Changes in stiffness vs tenocyte roundness in the 9% strain group over four hours of cyclic loading. A shows the declined proportion of cells with a spindle shape (Cat 4) compared with the declined stiffness. B shows the increase in the proportion of cells in the three remaining categories of roundness (Cat 3, Cat 2 and Cat 1) compared with the declined stiffness

Plotting changes in both mechanical characteristics (stiffness) against the Image-J circularity percentage indicate a solid concurrent morphological change with the loss of mechanical function (Figure 4). What is significant is that the proportion of spindle-like cells is related to the stiffness changes (controls). In contrast, the other three categories (individually) of elongation (circularity > 0.35) do not add any additional information about the mechanical changes. In the presence of GAG depletion, the proportion of spindle-shaped tenocytes occurs concurrently with immediate changes to stiffness. The control group has shown a decline in spindle-shaped tenocytes just before the linear decrease in stiffness and the proportion of spindle tenocytes.

4. DISCUSSION

This study has investigated the reliability and validity of a specific assessment of tendon morphology by employing the integrated data and pilot work of previous studies. This study has shown that the standard four-point ordinal classification systems for fibre structure, fibre orientation and arrangement and tenocyte shape are repeatable with high agreement using a double-blind testing protocol (26-29). Simple digital images can be randomly presented to the tester and, therefore, can assess the stability of observational classification protocols (single tester) over time. Biasutti *et al.* (2017) confirmed that ordinal scales created with four points on the tendon structure yield consistent results, hence the stability of single-tester observations on simple digital images (32). Nevertheless, the ordinal scale used in this context has limitations in proceeding with parametric statistical analysis because of its categorical nature. Thus, Chatterjee *et al.* (2023) suggest that experimental designs and inferential analysis are better borrowed by non-parametric approaches or by transforming ordinal data to a continuous measure. These findings underscore the necessity of rigorous descriptions of observational protocols and appropriate statistical tools in tendon morphology studies.

The second element of this study is that all four categorical (4-point) scoring systems (See supplementary & Table 1) have demonstrated an increase in the proportion of images that reflected increased damage. The observed relative shift in the proportion of the categorical scale reflects a dose-response effect. Namely, all three domains have demonstrated a concurrent increased 'damage' with the increased number of cycles (duration) and strain stimulus (increased from 3% to 9%). Consistent with the above findings, Edwards *et al.* (2018) argued that repeated exposure to strain stimuli leads to cumulative damage of the tendon (33). Therefore, these scales have clear face validity for the ordinal assessment of fibre structure, fibre orientation and arrangement and tenocyte shape. Notably, the proportion of the ordinal classifications for each block of images represented a sampling process. Also, Al Makhzoomi *et al.* (2021) elaborated that the variability of the values increases at each hour point

as the number of tendons in the imaging profile declines at each hour (26). As previously reported, this was caused by removing three tendons each hour for further histological assessments.

Further, the validity of the continuous assessment of tenocyte shape was analyzed from another study that only utilized two hours of testing at 6%. However, by pooling the same testing protocol from another study cohort (Figure 4), it is clear that the mechanical testing protocol was repeatable, and the decline in stiffness was consistent in different test cohorts undertaken at different times. The slight difference in the two control groups (A & B) clearly shows that the difference in the magnitude of the relative decline in the GAG-Depleted group was much more significant. Hussien *et al.* (2021) highlight the stability of the mechanical testing protocol. Therefore, greater confidence in the strength of the associations is shown between the tenocyte circularity and the decline in stiffness (35). Although Schöchlin et al. (2014) categorized the tenocyte shape, this study utilized the circularity threshold (24). The percentage of observed tenocyte cells was calculated for each image (at the full region of interest).
The number of cells varied; therefore, the total number was 100%. The percentage of long spindle-shaped tenocytes declines linearly with the decline in the overall tendon stiffness. The key finding is that this association was very strong for the category defined by the circularity of <0.35. In isolation, the other threshold categories of "elongated" 'oval' and "round" have similar or weaker associations with the mechanical changes. Notably, the control tendons slightly changed the proportion of spindle cells before a concomitant decline in stiffness. In contrast, the GAG-Depletion protocol demonstrated that the decline in the normalized proportion of spindle-shaped tenocytes was correlated very strongly with the decrease in tendon stiffness (26-28). In studies like Ilze Donderwinkel *et al.* (2022), GAG depletion protocols revealed a strong association between the degradation of spindle-shaped tenocytes and reduced tendon stiffness, particularly given that the circularity threshold was below 0.35 (36).

Although this study validates the categorical classification of tenocyte shape (both observational and digital), a key issue for future studies is finding a more sensitive circularity threshold by examining the possibility of adjusting the nominal circularity threshold. Also, investigating whether the strong linear association exists from zero cycles to complete rupture. This is important as these tendons were preconditioned by 720 cycles and managed under a strain (not stress) mediated protocol. In addition, a study by Franciele Dietrich-Zagonel et al. (2021) identified that preconditioning tendons with cyclic strains reduce cellular and mechanical properties (37). Although the subjective classification for fibre orientation and arrangement demonstrated a clear shift in categories over time, the digital data showed no changes after the significant preconditioning. By pooling similar data from different cohorts, it is clear that the digital assessment for anisotropy is reliable and differentiates between GAG depleted and controls after the preconditioning loading. Therefore, this experimental protocol's digital anisotropy and the observational classifications measure different domains. Although the digital image processing may be reliable, the validity for the context of the experimental protocol warrants further validation.
A further study area is to consider that this group of research papers utilized a strain-mediated repeated cyclic loading. The majority of the literature uses stress (load-mediated) fatigue protocol. The strain-mediate protocol meant that the load declined as the tendon failed; the alternative in the literature uses the same load, and then the strain (elongation) increases until rupture. The strain protocol was unique because this meant a much greater granularity of mechanical destruction happened over a greater cyclic period. The 720-cycle preconditioning cycles ensured that the tendons were fully prepared. The 720 would likely have had significant damage if this were a stress protocol. In this case, there were still issues because few and sometimes no images were considered to be "normal" in the randomly chosen images. It is unclear if the preconditioning caused very early substantial changes in the experiments, which were not recorded.

In summary, this is the first to report the reliability and validity of morphological measures for fibre structure, orientation arrangement and tenocyte shape. The ordinal classifications are repeatable and are seen to change as the objective evidence of mechanical failure is observed. The availability of objective digital imaging now provides some form of validation of classification systems and the opportunity to test stability in the assessment process in a double-blind protocol. Individuals need to be able to state the consistency in their observations to infer a substantial decrease in measurement bias. This study shows that the digital assessment of spindle-shaped tenocytes reflects the mechanical changes in the tendon. Digital processes should also be validated in the context that they may not need to replicate the four categorical constructs established previously in subjective assessment protocols. The findings of this study show that the continuous estimate of the percentage of spindle-shaped tenocytes (category 1, circularity <.0.35) in isolation is a strong predictor of mechanical changes. The other three categories may not add further information. It remains unclear if the 0.35 circularity model is the optimal cut-off. It would seem that the percentage of spindle tenocytes is also valid in GAG-depleted tendons with a significant decline in mechanical function. However, this may warrant further investigation with a less severe preconditioning effect.

5. CONCLUSION

This study has shown that the four categorical classification systems in tendon morphology are dose-sensitive and have face validity. The advent of digital platforms may lead to more reliable continuous and categorical data. Still, the algorithms' derivation is often from the qualitative framework underpinning the observations within the body of literature. Increased reliability is critical for experimental protocols, but the assumption that purports validity also needs to be tested. In this study, the tenocyte spindle shape is sensitive to mechanical changes, yet (unlike the observational categories) anisotropy was not. These replicated observations with different cohorts have demonstrated a stable testing protocol. These observations may manifest the strain protocol; therefore, future stress protocols would significantly add to this line of research.

Declaration and statement

Funding: No funding sources are reported

Ethical Approval: Not applicable

Conflict of interest: Authors do not have any conflict of interest.

Data availability statement: Data is available and will be provided at the editor's request.

Author Contributions: The authors have contributed to writing, designing, compiling, and editing the final manuscript.

REFERENCES

1. Hunter S, Werth J, James D, Lambrianides Y, Smith K, Karamanidis K, et al. Reliability and accuracy of a time-efficient method for the assessment of Achilles tendon mechanical properties by ultrasonography. Sensors. 2022;22(7):2549.
2. Firminger CR, Edwards WB. Effects of cyclic loading on the mechanical properties and failure of human patellar tendon. Journal of Biomechanics. 2021;120:110345.
3. Hugh E. Measurement of tendon transverse stiffness in people with Achilles tendinopathy: a cross-sectional study. 2018.
4. Buffey AJ, Onambélé-Pearson GL, Erskine RM, Tomlinson DJ. The validity and reliability of the Achilles tendon moment arm assessed with dual-energy X-ray absorptiometry, relative to MRI and ultrasound assessments. Journal of Biomechanics. 2020;116:110204.
5. Masic A, Bertinetti L, Schuetz R, et al. Observations of multi-scale, stress-induced changes of collagen orientation in tendon by polarized Raman spectroscopy. Biomacromolecules. 2011 Nov;12(11):3989-96.
6. Miller KS, Connizzo BK, Feeney E, Soslowsky LJ. Characterizing local collagen fiber re-alignment and crimp behavior throughout mechanical testing in a mature mouse supraspinatus tendon model. Journal of Biomechanics. 2012 Aug;45(12):2061-5.
7. Franchi M, Raspanti M, Dell'Orbo C, et al. Different crimp patterns in collagen fibrils relate to the subfibrillar arrangement. Connective Tissue Research. 2008;49(2):85-91.
8. Hurschler C, Provenzano PP, Vanderby R Jr. Scanning electron microscopic characterization of healing and normal rat ligament microstructure under slack and loaded conditions. Connective Tissue Research. 2003;44(2):59-68.
9. Matyas J, Edwards P, Miniaci A, et al. Ligament tension affects nuclear shape in situ: an in vitro study. Connective Tissue Research. 1994;31(1):45-53.
10. Screen HR, Lee DA, Bader DL, Shelton JC. Development of a technique to determine strains in tendons using the cell nuclei. Biorheology. 2003;40(1-3):361-8.
11. Thorpe CT, Chaudhry S, Lei II, et al. Tendon overload results in alterations in cell shape and increased markers of inflammation and matrix degradation. Scandinavian Journal of Medicine & Science in Sports. 2015 Aug;25(4):e381-91.
12. Lake SP, Miller KS, Elliott DM, Soslowsky LJ. Effect of fiber distribution and realignment on the nonlinear and inhomogeneous mechanical properties of human supraspinatus tendon under longitudinal tensile loading. Journal of Orthopaedic Research. 2009 Dec;27(12):1596-602.
13. Arnoczky SP, Lavagnino M, Whallon JH, Hoonjan A. In situ cell nucleus deformation in tendons under tensile load; a morphological analysis using confocal laser microscopy. Journal of Orthopaedic Research. 2002 Jan;20(1):29-35.
14. Magra M, Maffulli N. Genetic aspects of tendinopathy. Journal of Science and Medicine in Sport. 2008 Jun;11(3):243-7.
15. Voleti PB, Buckley MR, Soslowsky LJ. Tendon healing: repair and regeneration. Annual Review of Biomedical Engineering. 2012;14:47-71.
16. Szczesny SE, Elliott DM. Incorporating plasticity of the interfibrillar matrix in shear lag models is necessary to replicate the multi-scale mechanics of tendon fascicles. Journal of the Mechanical Behavior of Biomedical Materials. 2014 Dec;40:325-38.

17. Fung DT, Wang VM, Andarawis-Puri N, et al. Early response to tendon fatigue damage accumulation in a novel in vivo model. Journal of Biomechanics. 2010;43(2):274-9.
18. Chen J, Yu Q, Wu B, et al. Autologous tenocyte therapy for experimental Achilles tendinopathy in a rabbit model. Tissue Engineering Part A. 2011 Aug;17(15-16):2037-48.
19. Kartus J, Movin T, Papadogiannakis N, Christensen LR, Lindahl S, Karlsson J. A radiographic and histologic evaluation of the patellar tendon after harvesting its central third. The American Journal of Sports Medicine. 2000 Mar;28(2):218-26.
20. Movin T, Gad A, Reinholt FP, Rolf C. Tendon pathology in long-standing achillodynia: biopsy findings in 40 patients. Acta Orthopaedica Scandinavica. 1997 Apr;68(2):170-5.
21. Movin T. Aspects of aetiology, pathoanatomy and diagnostic methods in chronic mid-portion achillodynia. 1999.
22. Maffulli N, Barrass V, Ewen SW. Light microscopic histology of Achilles tendon ruptures: A comparison with unruptured tendons. American Journal of Sports Medicine. 2000 Nov-Dec;28(6):857-63.
23. Xu Y, Murrell GA. The basic science of tendinopathy. Clinical Orthopaedics and Related Research. 2008 Jul;466(7):1528-38.
24. Schöchlin M, Weissinger SE, Brandes AR, Herrmann M, Möller P, Lennerz JK. A nuclear circularity-based classifier for diagnostic distinction of desmoplastic from spindle cell melanoma in digitized histological images. Journal of Pathology Informatics. 2014;5(1):40.
25. Dickson DM, Fawole HO, Newcombe L, Smith SL, Hendry GJ. Reliability of ultrasound strain elastography in the assessment of the quadriceps and patellar tendon in healthy adults. Ultrasound. 2019.
26. Al Makhzoomi AK, Kirk TB, Allison GT. A multi-scale study of morphological changes in tendons following repeated cyclic loading. Journal of Biomechanics. 2021 Nov 9;128:110790.
27. Al Makhzoomi AK, Kirk TB, Allison GT. An AFM study of the nanostructural response of New Zealand white rabbit Achilles tendons to cyclic loading. Microscopy Research and Technique. 2022 Feb;85(2):728-37.
28. Al Makhzoomi AK, Kirk TB, Dye DE, Allison GT. Contribution of glycosaminoglycans to the structural and mechanical properties of tendons: A multi-scale study. Journal of Biomechanics. 2021 Nov 9;128:110796.
29. Al Makhzoomi AK, Kirk TB, Dye DE, Allison GT. The influence of glycosaminoglycan proteoglycan side chains on tensile force transmission and the nanostructural properties of Achilles tendons. Microscopy Research and Technique. 2022 Jan;85(1):233-43.
30. Park MS, Kang KJ, Jang SJ, Lee JY, Chang SJ. Evaluating test-retest reliability in patient-reported outcome measures for older people: A systematic review. International Journal of Nursing Studies. 2017;79:58-69.
31. Landis JR, Koch GG. The measurement of observer agreement for categorical data. Biometrics. 1977 Mar;33(1):159-74.
32. Biasutti S, Dart A, Smith M, Blaker C, Clarke E, Jeffcott L, et al. Spatiotemporal variations in gene expression, histology, and biomechanics in an ovine model of tendinopathy. PLoS ONE. 2017;12:e0185282.
33. Chatterjee M, Evans MK, Bell R, Nguyen PK, Kamalitdinov TB, Korntner S, et al. Histological and immunohistochemical guide to tendon tissue. Journal of Orthopaedic Research. 2023;41:2114-32.
34. Edwards WB. Modeling overuse injuries in sport as a mechanical fatigue phenomenon. Exercise and Sport Sciences Reviews. 2018;46:224-31.
35. Hussien AA, Knell R, Renoux F, Wunderli SL, Niederoest B, Foolen J, et al. Sustained mechanical tension governs fibrogenic activation of tendon stromal cells in systemic sclerosis. bioRxiv. 2021.
36. Donderwinkel I, Tuan RS, Cameron NR, Frith JE. Tendon tissue engineering: Current progress towards an optimized tenogenic differentiation protocol for human stem cells. Acta Biomaterialia. 2022;145:25-42.
37. Dietrich-Zagonel F, Hammerman M, Bernhardsson M, Eliasson P. Effect of storage and preconditioning of healing rat Achilles tendon on structural and mechanical properties. Scientific Reports. 2021;11.